Int J Theor Phys (2010) 49: 276–292
DOI 10.1007/s10773-009-0201-0

Quantum Entropy of a Nonlinear Two-level Atom with Atomic Motion

M.S. Ateto

Received: 31 March 2009 / Accepted: 23 November 2009 / Published online: 9 December 2009

Abstract The wave function of a system governed by the time-dependent nonlinear Jaynes-Cummings (JC) model is obtained. We compute analytically the eigenvalues of the reduced field density operator by which the dynamics of the entropy of entanglement of the cavity field are analyzed. The influences of the atomic motion, the field-mode structure and the Kerr-like medium on this phenomenon are illustrated. The population dynamics of an excited atom is also discussed for the same set of parameters. The cavity field is assumed to be initially excited in either a Fock or a coherent states. The cavity excitation in a Fock state generates a class of an entanglement without death with fixed amplitude by adjusting the parameters of the atomic motion as well as the Kerr and the field-mode structure. In case of a coherent cavity, the only phenomenon to be noted is the periodical behavior of the dynamics under study when the atomic motion is considered. Although the Kerr medium affects the strength of the entanglement negatively, the entropy of entanglement loses its zeros where the Kerr is taken into consideration.

Keywords Entropy · Atomic motion · Field-mode structure · Nonlinear medium · Coherent field

1 Introduction

Laser cooling and atomic trapping technologies make it necessary to consider the atomic motion in preparing the cool or super cool atoms. Recently, the atomic space motion has been taken into consideration in order to achieve cooled atoms and the super-cooled atoms with the technology of laser cooling and trapped atoms technology [1]. The researches

Present address:
M.S. Ateto (✉)
Mathematics Department, Faculty of Science at Qena, South Valley University, 83523 Qena, Egypt
e-mail: omersog@yahoo.com

M.S. Ateto
Theoretisch-Physikalisches Institut, Friedrich-Schiller-Universität Jena, Max-Wien-Platz 1, 07743 Jena, Germany

showed that the atomic motion can bring about the nonlinear effect of atomic population [2–4] and enhance the fidelity of quantum state [5]. Furthermore, it has become an active research subject to prepare squeezed light using the interaction between the photon field and atom [6] which has potential application in detecting weak signals and light communications. Recently, the effect of the atomic motion and field-mode structure on entanglement attracted much attention [7–9]. Entanglement is one of the most intriguing features of Quantum Mechanics (QM) and in the early times of QM it was recognized by Erwin Schrödinger [10] and by Einstein, Podolsky and Rosen [11]. These purely quantum correlations play a fundamental role in modern physics and in recent years the interest in entanglement has increased considerably. First because it is a fundamental tool in Quantum Information Theory and a consistent characterization of its theoretical properties is needed. Second because the present stage of technology permits us to perform some experimental manipulations with it in quantum information processing and communication [12], such as Quantum Teleportation [13, 14], Quantum Cryptography [15, 16], Quantum Dense Coding [17], and Quantum Computation [18, 19]. Therefore, it is of great importance to quantify entanglement to assess the efficacy the quantum information processing. One of the key problems in entanglement study is the generation and manipulation of quantum entangled states. At present, entanglement of two-level systems has been used to represent information in most quantum information processing. A great effort has been devoted in quantifying entanglement involving various methods and interesting concepts [20–37]. However, the degree of quantum entanglement depends crucially on the physical nature of the interacting objects and the character of their mutual coupling. It has been noticed that all these study results have been obtained for the case where either the nonlinear medium or the atomic motion is ignored. The Kerr medium can be modelled as an anharmonic oscillator with frequency Ω. Physically this model may be realized as if the cavity contains two different species of atoms, one of which behaves like a two-level atom and the other behaves like an anharmonic oscillator in the single-mode field of frequency Ω [38]. The cavity mode is coupled to the Kerr medium as well as to the two-level atoms. The Kerr-like medium can be useful in many aspects, such as detection of nonclassical states [39], quantum nondemolition measurement [40], investigation of quantum fluctuations [41], generation of entangled macroscopic quantum states [42, 43], and quantum information processing [44, 45].

In this paper we present a treatment into another direction. We examine the effects of the atomic motion and the field-mode structure on the atom-field entanglement when the cavity field assumed to be filled with a nonlinear Kerr-like medium contained inside a very good quality cavity via one-quantum transition process. The analytical solution for the problem under consideration, namely, the eigenvalues and eigenfunctions for the time-dependent nonlinear (JC) model are obtained. By using the solutions obtained, we investigate the properties of the field entropy and atom-field entanglement. In Sect. 2 we present the generalized model and derive the time-dependent wave function of the total system when the field eigenfrequency is assumed to be on- and off-resonance with the atomic transition. Depending on this wave function, the reduced field density operator is also derived. The eigenvalues of the reduced field density operator and the final form of the entropy of field entanglement are computed and showed in Sect. 3. Section 4 includes the final expression of the atomic population which we are going to use in the present work. The numerical calculations supported by the discussion of the numerical results are presented in Sect. 5. Our concluding remarks are showed in Sect. 6.

2 Model

We start from the extended (JC) Hamiltonian

$$\hat{H}(z) = \Omega a^{\dagger}a + \frac{\omega}{2}\sigma + \chi a^{\dagger}a(a^{\dagger}a - 1) + 2\sqrt{\chi}a^{\dagger}a + \lambda f(z)(a^{\dagger}\sigma_{01} + a\sigma_{10}), \tag{1}$$

and the wave function of the full system in the form

$$|\psi(t)\rangle = \sum_{k=0} C_k[a_k(t)|1,k\rangle + b_{k+1}(t)|0,k+1\rangle]. \tag{2}$$

The Hamiltonian (1) can be written in the form

$$\hat{H} = \hat{H}_0 + \hat{H}_{INT}, \tag{3}$$

with $\hat{H}_0$ being the unperturbated Hamiltonian

$$\hat{H}_0 = \hat{H}_{atom} + \hat{H}_{field} = \Omega\left(a^{\dagger}a + \frac{\sigma}{2}\right), \tag{4}$$

and $\hat{H}_{INT}$ being the atom-field interaction Hamiltonian

$$\hat{H}_{INT}(t) = \frac{\Delta}{2}\sigma + \chi a^{\dagger}a(a^{\dagger}a - 1) + 2\sqrt{\chi}a^{\dagger}a + \lambda f(vt)(a|e\rangle\langle g| + |g\rangle\langle e|a^{\dagger}), \tag{5}$$

$$\Delta = \omega - \Omega. \tag{6}$$

The states $|1\rangle$ and $|0\rangle$ denote the upper and lower atomic states. We denote by $|jk\rangle \equiv |j\rangle_A \otimes |k\rangle_F$ the eigenstates of $\hat{H}_0$ showing that the atom (A) is in the unperturbated quantum state j and the field carries k photon ($i \in \{0,1\}$, $k = 0,1,2,3,\ldots$). The well known raising, lowering and population operators are respectively, $\sigma_{10} = |1\rangle\langle 0|$, $\sigma_{01} = \sigma_{10}^{\dagger}$ and $\sigma = |1\rangle\langle 1| - |0\rangle\langle 0|$. The operators a and $a^{\dagger}$ denote respectively the well-known annihilation and creation operators of the field-mode of frequency Ω. We denote by χ the dispersive part of the third order nonlinearity of Kerr-like medium [46–48]. The coupling constant λ is essentially the product of the atomic transition matrix element and the electric field "per photon" and $f(z)$ is the shape function of the cavity field mode.

We restrict our self for the atomic motion along the z axis, so that only z-dependence of the field mode function was taken into account. The function $f(z)$ is given by [4, 8, 9, 49, 50, 56]

$$f(z) \to f(vt) = \sin(p\pi vt/L), \tag{7}$$

however, we may describe it in the present work by

$$f(z) \to f(vt) = \cos(p\pi vt/L), \tag{8}$$

where v is the atomic motion velocity and p is a positive integer representing the number of half wavelengths of the field mode inside a cavity of length L.

The dynamics of the system are determined for each value of n by two coupled nonlinear differential equations for the complex amplitudes $a_k(t)$ and $b_{k+1}(t)$. Alternatively, at any

time $t > 0$ the joint state vector of the field and the first atom can be obtained from the time-dependent analytical solution of the Schrödinger equation

$$i\frac{d}{dt}|\psi_{AF}(t)\rangle = H_{INT}|\psi_{AF}(t)\rangle. \tag{9}$$

Let the atom undergoing one-photon transition being in its upper state $|e\rangle$ going through a cavity in a superposition of the number state

$$|\psi_F(0)\rangle = \sum_{k=0} C_k|k\rangle, \tag{10}$$

then the initial state vector of atom-field system is given by

$$|\psi_{AF}(0)\rangle = |\psi_A(0)\rangle \otimes |\psi_f(0)\rangle = \sum_{k=0} C_k|k,1\rangle. \tag{11}$$

The atom leaves the cavity again after passing p half-wavelengths of the electric field, the wave vector of the full system at any time $t > 0$ is given by (2). Applying the Schrödinger (9), we obtain the couple nonlinear ordinary differential equations

$$\frac{da_k(t)}{dt} = -i\gamma_1(k)a_k(t) - ig(k+1,t)b_{k+1}, \tag{12}$$

$$\frac{db_{k+1}(t)}{dt} = -i\gamma_2(k+1)b_{k+1}(t) - ig(k+1,t)a_k, \tag{13}$$

with

$$\gamma_1(k) = \frac{\Delta}{2} + \chi k(k-1) + 2\sqrt{\chi}k, \tag{14}$$

$$\gamma_2(k+1) = -\frac{\Delta}{2} + \chi k(k+1) + 2\sqrt{\chi}(k+1) \tag{15}$$

and

$$g(k+1,t) = \lambda\sqrt{k+1}\,f(vt). \tag{16}$$

When we let $p \to 0$ in the above formulae we obtain the case of rest atom.

For arbitrary $g(t)$ the coupled differential equation have in general no exact solution, but under some certain conditions the solution can be found.

2.1 Linear On-resonance Solution

Assuming that the Kerr medium is absent, namely, $\chi = 0$ and the cavity eigenfrequency is on resonance with the atomic transition, i.e., $\Delta = 0$, in this case we have $\gamma_1 = \gamma_2 = 0$. As a result, the couple nonlinear equations (12) and (13) reduces to a couple of linear ordinary differential equations which can be easily solved. The solution of these modified set of equations resulted in the complex amplitudes $a_k(t)$ and $b_{k+1}(t)$ as

$$a_k(t) = \cos(\lambda\sqrt{k+1}\Theta(t)), \tag{17}$$

$$b_{k+1}(t) = -i\sin(\lambda\sqrt{k+1}\Theta(t)), \tag{18}$$

where, for a particular experimentally-possible choice of the atomic motion $v = \lambda L/\pi$ [2, 4, 50], the function $\theta(t)$ is given by

$$\Theta(t) = \int_0^t f(vt')dt' = \frac{1}{p\lambda}\sin(p\lambda t). \tag{19}$$

2.2 Nonlinear Off-resonance Solution

In this case, the field eigenfrequency is assumed to be far-off-resonance from the atomic transition, and the cavity field assumed to be filled with the nonlinear Kerr-like medium. The problem at this stage is to solve the couple nonlinear differential equations (12) and (13) in terms of the conditions indicated above.

To do this, it is convenient to define the operators

$$a_k(t) = V_k(t)\exp\left[i\left(\frac{x(k+1,t)}{2} - \gamma_1(k)t\right)\right], \tag{20}$$

$$b_{k+1}(t) = W_{k+1}(t)\exp\left[-i\left(\frac{x(k+1,t)}{2} + \gamma_2(k+1)t\right)\right], \tag{21}$$

where

$$x(k+1,t) = -[\gamma_2(k+1) - \gamma_1(k)]t. \tag{22}$$

Substitution of these operators into (12) and (13) gives the couple first-order nonlinear differential equations

$$\frac{dV_k(t)}{dt} = -i\frac{\dot{x}(k+1,t)}{2}V_k(t) - ig(k+1,t)W_{k+1}(t), \tag{23}$$

$$\frac{dW_{k+1}(t)}{dt} = i\frac{\dot{x}(k+1,t)}{2}W_{k+1}(t) - ig(k+1,t)V_k(t), \tag{24}$$

where, $\dot{x} = \frac{dx}{dt}$.

Employing the transformation

$$[V] = [X]\cdot[V], \tag{25}$$

where,

$$[V] = \begin{bmatrix} V(t) \\ W(t) \end{bmatrix}, \tag{26}$$

$$[X] = \begin{bmatrix} \cos[\varrho(k+1,t)] & \sin[\varrho(k+1,t)] \\ -\sin[\varrho(k+1,t)] & \cos[\varrho(k+1,t)] \end{bmatrix}, \tag{27}$$

and,

$$[V_1] = \begin{bmatrix} V_1(t) \\ W_1(t) \end{bmatrix}, \tag{28}$$

and after minor algebra, we obtain the couple second-order homogeneous differential equations with time-dependent coefficients

$$\frac{d^2V_1(t)}{dt^2} - \Omega_1(k+1,t)\frac{dV_1(t)}{dt} + \Lambda(k+1,t)V_1(t) = 0, \tag{29}$$

$$\frac{d^2W_1(t)}{dt^2} - \Omega_2(k+1,t)\frac{dV_1(t)}{dt} + \Lambda(k+1,t)W_1(t) = 0, \tag{30}$$

where

$$\Omega_1(t) = \frac{\ddot{\varrho}(t) + i\dot{\varepsilon}(t)}{\dot{\varrho}(t) + i\varepsilon(t)}, \tag{31}$$

$$\Omega_2(t) = \frac{\ddot{\varrho}(t) - i\dot{\varepsilon}(t)}{\dot{\varrho}(t) - i\varepsilon(t)}, \tag{32}$$

$$\Lambda(t) = (\dot{\varrho}(t))^2 + \varepsilon^2(t), \tag{33}$$

with

$$\tan[2\varrho(k+1,t)] = \frac{\dot{x}(k+1,t)}{2g(k+1,t)}, \tag{34}$$

$$\varepsilon(k+1,t) = g(k+1,t)\sec[2\varrho(k+1,t)], \tag{35}$$

where $\dot{\vartheta} = \frac{d\vartheta}{dt}$ and $\ddot{\vartheta} = \frac{d^2\vartheta}{dt^2}$; $\vartheta = \varrho$ or ε.

To solve the couple second-order homogeneous differential equations with time-dependent coefficients (29) and (30), let us introduce the integrability condition

$$\frac{\dot{x}(k+1,t)}{2g(k+1,t)} = \frac{2\alpha Y(k+1,t)+\beta}{\sqrt{1-(2\alpha Y(k+1,t)+\beta)^2}}, \tag{36}$$

where α and β are arbitrary constants and

$$Y(k+1,t) = \int g(k+1,t')dt'. \tag{37}$$

Employing the integrability condition (36), we can express the general solution of couple first-order differential equations (23) and (24) in the following form

$$\begin{aligned} V_k(t) = {} & \cos[Z(k+1,t)]\cos[\mu(k+1,t)] \\ & - \frac{i}{2}\frac{[\gamma_1(k)-\gamma_2(k+1)]\sin[Z(k+1,t)]\cos[\mu(k+1,t)]}{\dot{Z}(k+1,0)} \\ & - i\frac{\lambda\sqrt{k+1}\sin[Z(k+1,t)]\sin[\mu(k+1,t)]}{\dot{Z}(k+1,0)} \\ & + \frac{\dot{\varrho}(k+1,0)\sin[Z(k+1,t)]\sin[\mu(k+1,t)]}{\dot{Z}(k+1,0)}, \end{aligned} \tag{38}$$

$$\begin{aligned} W_{k+1}(t) = {} & -\cos[Z(k+1,t)]\sin[\mu(k+1,t)] \\ & + \frac{i}{2}\frac{[\gamma_1(k)-\gamma_2(k+1)]\sin[Z(k+1,t)]\sin[\mu(k+1,t)]}{\dot{Z}(k+1,0)} \end{aligned}$$

$$-i\frac{\lambda\sqrt{k+1}\sin[Z(k+1,t)]\cos[\mu(k+1,t)]}{\dot{Z}(k+1,0)}$$
$$+\frac{\dot{\varrho}(k+1,0)\sin[Z(k+1,t)]\cos[\mu(k+1,t)]}{\dot{Z}(k+1,0)}, \tag{39}$$

with

$$Z(k+1,t)=\sqrt{\alpha^2+1}\int_0^t \varepsilon(k+1,t')dt', \tag{40}$$

$$\mu(k+1,t)=\varrho(k+1,t)-\varrho(k+1,0), \tag{41}$$

recalling the operators (20) and (21) with the (38)–(41), we obtain the complex amplitudes $a_k(t)$ and $b_{k+1}(t)$.

However, the wave function of the full system is obtained, any property related to the atom or the field can be calculated. The reduced density operators can be written as

$$\rho_{A(F)}=\mathrm{Tr}_{F(A)}\,|\psi(t)\rangle\langle\psi(t)|, \tag{42}$$

and we have used the subscript $A(F)$ to denote the atom (field). By using equation (2) the reduced field density operator takes the form

$$\rho_F(t)=\sum_{k,l} C_k C_l^*(\rho_{kl}|k\rangle\langle l|+\rho_{k+1l+1}|k+1\rangle\langle l+1|)=|R_1\rangle\langle R_1|+|R_2\rangle\langle R_2|, \tag{43}$$

where,

$$|R_1\rangle=\sum_{k=0} C_k\rho_k(t)|k\rangle, \tag{44}$$

$$|R_2\rangle=\sum_{k=0} C_k\rho_{k+1}(t)|k+1\rangle, \tag{45}$$

with,

$$\rho_{kl}(t)=\rho_k(t)\rho_l^*(t)=a_k(t)a_l^*(t), \tag{46}$$

$$\rho_{k+1l+1}(t)=\rho_{k+1}(t)\rho_{l+1}^*(t)=b_{k+1}(t)b_{l+1}^*(t). \tag{47}$$

3 Quantum Entropy

The dynamics described by the Hamiltonian (1) leads to an entanglement between the field and the atom. In order to calculate the entropy $S_F(t)$, we must obtain the eigenvalues of the reduced field density operator. Employing the reduced density operator for the field given by (43), we investigate the properties of the entropy S_F and entanglement in the framework of time-dependent nonlinear (JC) model. Quantum mechanically, the entropy is defined as

$$S=-K\,\mathrm{Tr}\,\rho\ln\rho, \tag{48}$$

where ρ is the density operator for a given quantum system and K represents Boltzmann's constant. If ρ describes a pure state, then $S=0$ and if ρ describes a mixed state, then $S\neq 0$.

The entropies of the atom and the field, when treated as a separate system, are defined through the corresponding reduced density operator by

$$S_{A(F)} = -\operatorname{Tr}_{A(F)}[\rho_{A(F)} \ln \rho_{A(F)}]. \tag{49}$$

In order to derive a calculation formalism of the field entropy, we must obtain the eigenvalues of the reduced field density operator given by (43). According to the general method of Pheonix and Knight [51–53], the eigenvalues of the reduced field density operator (43), reads

$$\Pi^{+} = \frac{1}{2}(1 + \sqrt{(\langle R_1|R_1\rangle - \langle R_2|R_2\rangle)^2 + 4|\langle R_1|R_2\rangle|^2}), \tag{50}$$

$$\Pi^{-} = \frac{1}{2}(1 - \sqrt{(\langle R_1|R_1\rangle - \langle R_2|R_2\rangle)^2 + 4|\langle R_1|R_2\rangle|^2}). \tag{51}$$

In terms of the eigenvalues (50) and (51), the field entropy expressed as

$$S_F(t) = -\Pi^{+} \ln \Pi^{+} - \Pi^{-} \ln \Pi^{-}. \tag{52}$$

4 Population

Atomic population inversion is an important atomic observable in the two-level system which is defined as the difference between the probabilities of finding the atom in the excited state and in the ground state. The atomic inversion $P(t)$ of the model under consideration is given by the expression

$$\begin{aligned} P(t) &= \langle R_1|R_1\rangle - \langle R_2|R_2\rangle \\ &= \sum_k |C_k|^2(\rho_{kk} - \rho_{k+1k+1}) = \sum_k |C_k|^2(|a_k(t)|^2 - |b_{k+1}(t)|^2). \end{aligned} \tag{53}$$

5 Results of Calculations

On the basis of the analytical solutions presented in the previous sections, we shall examine the dynamics of both the field entropy $S_F(t)$ and the atomic population $P(t)$. For all our plots the detuning parameter are adjusted such that $\Delta = 0$, i.e., the cavity eigenfrequency is on resonance with the atomic transition frequency. To get clearer insight about the situation, we consider the cavity field is excited initially in two different states, namely, a Fock state and a coherent state where a comparison between the results of the two states will be analyzed.

5.1 The Cavity Is Excited in the Fock State

For Fock state field, the amplitudes C_k in (10) obey the delta function relation

$$C_k = \delta_{kl}, \tag{54}$$

where l is the photon number of Fock state.

By setting $C_k = \delta_{kl}$ in (11), we obtain the state vector of the full system in a Fock state. In order to appreciate some different situations, we show in what follows some plots of field

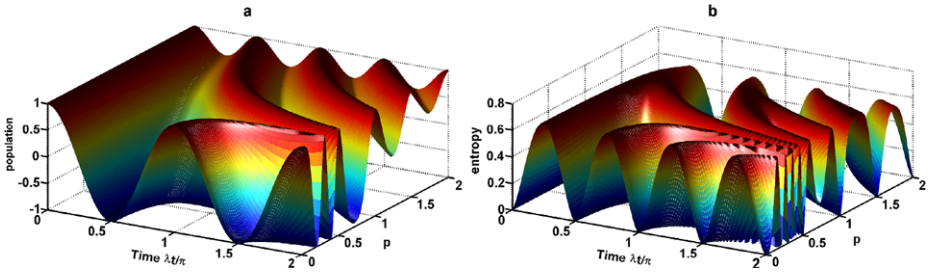

Fig. 1 The evolution of field entropy $S_F(t)$ and the population $P(t)$ as functions of the scaled time $\lambda t/\pi$ and the field-mode structure p for vacuum cavity field $|0\rangle$ where (**a**) the population $P(t)$ (**b**) the field entropy S_F

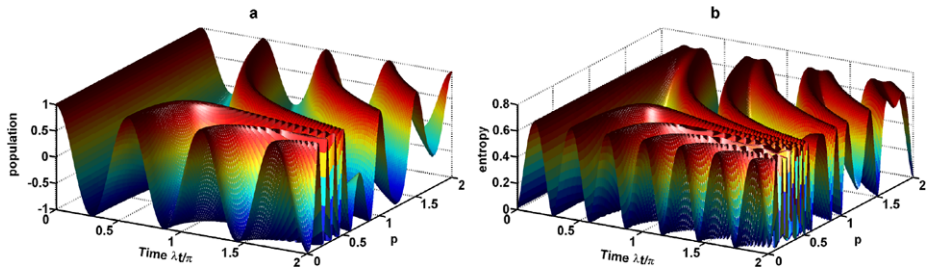

Fig. 2 The same as Fig. 1, but when the cavity is excited with two field quanta $\langle 2\rangle$

entropy $S_F(t)$ and the corresponding population $P(t)$ for different values of the involved parameters. Using the Fock state as an initial state of the field, the dependence of S_F on the scaled time $\lambda t/\pi$ and the field mode structure parameter p is shown in Figs. 1 and 2 for the Fock states $|0\rangle$ and $|1\rangle$, respectively. The general behavior of both S_F and P due to the field-Fock-state contains no surprise; the value of the entropy S_F at first is zero, which is quite remarkable, while the value of P is 1, regardless of the value of the parameter p (see Fig. 1). This is due to at $\lambda t = 0$, the field and the excited atom $P(t = 0) = 1$ are separable, namely, in pure state $S_F(t = 0) = 0$. The case of the effective vacuum $n = 0$ and for rest atoms $p = 0$ is quite interesting. In this case S_F as well as P oscillate periodically between zero and their maxima. The periods lay at $\lambda t = n\pi/2$ and $\lambda t = n\pi$, $n = 0, 1, 2, 3, \ldots$ for S_F and P, respectively. We notice clearly that the periods of P are twice that of the entropy S_F. This periodical evolution is preserved as long as time goes on. As the parameter p going to increase slightly, specially for small values such as $p < 1$, the entropy of the field S_F as well as the population P lose some of their zeros except for some instants at which S_F and P reach their minima. This means that in the interval $0 < p < 1$ the atom and the field become strong entangled for long periods of time. It is worth to mention that the periods of oscillation of P are also twice that of S_F as long as $p < 1$. As the parameter p is considerably increased such as $p > 1$, the entropy S_F goes to zeros lately with periods equal to that of P till $p = 2$, at which both S_F and P have exactly the same periods. In this case the field entropy S_F oscillates between zeros and its maximum value 1/2, while P oscillates between the values $P = 1/2$ and $P = 1.0$ as we can notice clearly from Fig. 1a. It is clear that the field and the atom are in maximum entangled state at the instants when the atom is in its superposition state $|\psi(t)\rangle = \frac{1}{\sqrt{2}}(|1\rangle + |0\rangle)$.

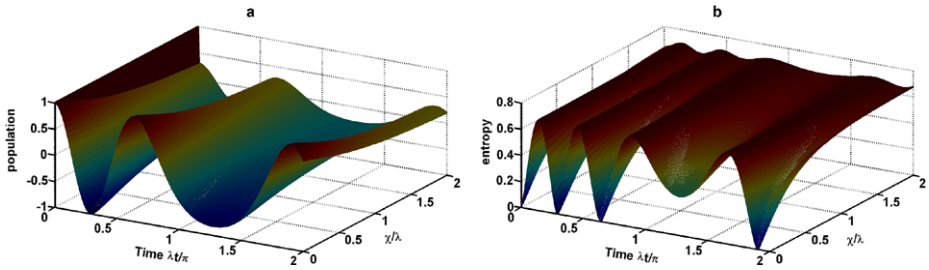

Fig. 3 The evolution of field entropy $S_F(t)$ and the population $P(t)$ as functions of the scaled time $\lambda t/\pi$ and the Kerr medium parameter χ/λ when the cavity is excited with two field quanta $\langle 2\rangle$ and the field-mode structure parameter $p = \pi/8$ where (**a**) the population $P(t)$ (**b**) the field entropy S_F

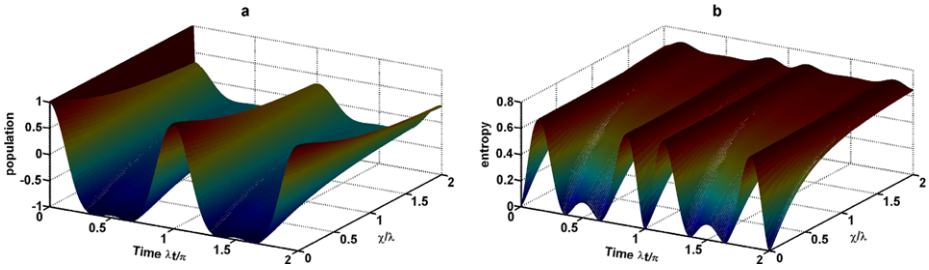

Fig. 4 The same as Fig. 3, but for $p = 1$

The shape of the functions $S_F(t)$ and $P(t)$ look like sand dunes. As the number of excitation increases $n = 2$, the number of oscillation increases (see Fig. 2), while the general behavior of both S_F and P is preserved.

To discuss the effect of the Kerr-like medium in the presence of the atomic motion, we have plotted several figures for the functions S_F and P against the scaled time $\lambda t/\pi$ and the Kerr parameter χ/λ for different values of the mode-field structure parameter p. In our computational program we adjusted the field-mode structure $p = \pi/8$, 1 and 2 in Figs. 3, 4 and 5, respectively. Generally at $\chi/\lambda = 0$, the previous behavior is preserved where S_F as well as P oscillate between zero and their maxima but with longer periods of time start shorter at $\lambda t < 0.6\pi$. It is clearly remarkable that for all values of λt the entropy is only zero for rest atoms, while long-lived correlated states—with approximately fixed amplitude—between the atom and the field are observed as p goes on increasing for all time stages. Furthermore, for high values of p, the degree of entanglement does not depend crucially on the population behavior as previous case where the Kerr medium is neglected (see Figs. 3, 4 and 5), specially when $\chi/\lambda = 2$. When the Kerr is ignored and $p = 1$, we notice clearly more periods appear in the same interval of time. Additionally, closed periods appear more clearly than previous with periods lay at $\lambda t = n\pi$, $n = 0, 1, 2, 3, \ldots$ for both S_F and P. On the increasing of χ/λ the long-lived entanglement between the field and the atom is observed with slight oscillated behavior in half of the revival time. Additionally, we notice more closer periodical oscillations between zero and the maximum values in the behavior of both S_F and P in all time stages when the Kerr medium is absent. Again for all values of $\lambda t/\pi$, the entropy is only zero for rest atoms, while long-lived entangled states are observed with approximately fixed amplitude when p reaches the value 2.

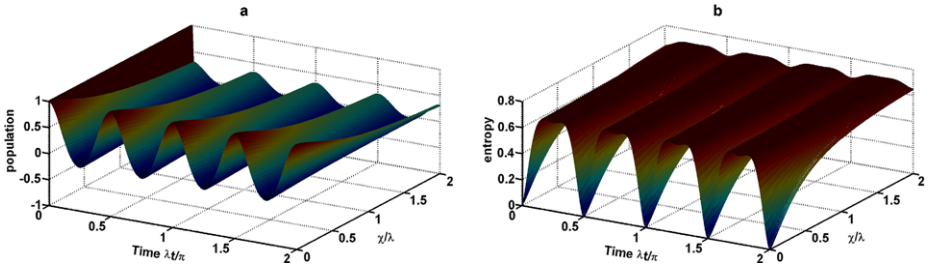

Fig. 5 The same as Fig. 3, but for $p = 2$

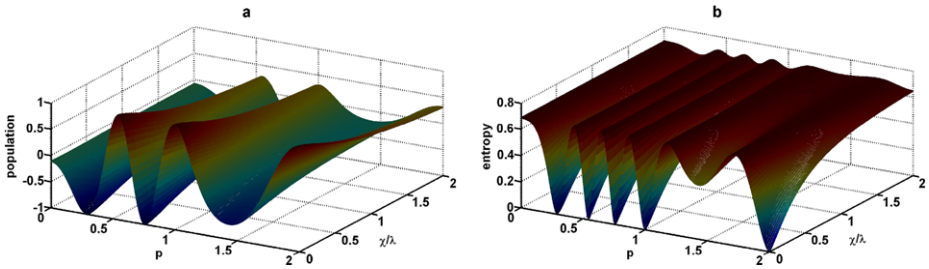

Fig. 6 The evolution of field entropy $S_F(t)$ and the population $P(t)$ as a functions of the field-mode structure p and the Kerr medium parameter χ/λ when the cavity is excited with two field quanta $\langle 2\rangle$ and the scaled time $\lambda t = \pi$ where (**a**) the population $P(t)$ (**b**) the field entropy S_F

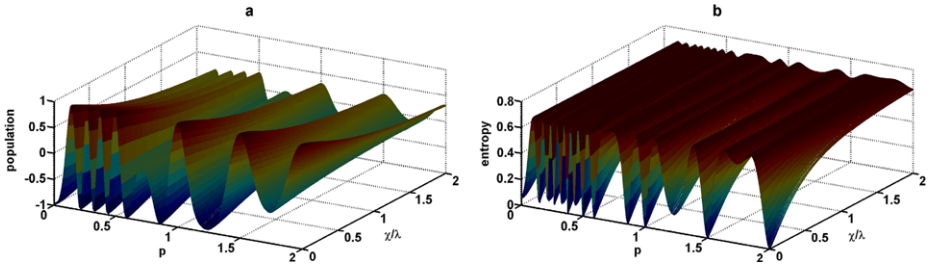

Fig. 7 The same as Fig. 6, but for $\lambda t = 2\pi$

To get clearer insight about the results, we have plotted the field entropy S_F as well as the population P as functions of the field-mode structure parameter p and the Kerr parameter χ/λ for different values of the scaled time $\lambda t/\pi$. This is illustrated in Figs. 6 and 7 where $\lambda t = \pi$ and $\lambda t = 2\pi$. For small values of p, we notice that the oscillations of both the entropy S_F and the population P are between zero and their maxima when the Kerr medium is absent. As the parameter χ/λ going to increase, we notice clearly the long-lived entangled states of the field and the atom which does not depend at all on the population value (see Fig. 6). This behavior was noticed before (see Fig. 3). At the next time stage when $\lambda t = 2\pi$, the closer oscillations between zero and the maximum values appear in the interval $p \in [0, 0.6[$ regardless of the value of χ/λ, while in the interval $p \in]0.6, 2]$ the long-lived atom-field entanglement is observed again for strong Kerr medium where $\chi/\lambda = 2$ (see Fig. 7).

5.2 The Cavity Is Excited in the Coherent State

We devote this subsection to numerically calculate the atom-field entanglement measured via the entropy $S_F(t)$ as well as the corresponding population $P(t)$ when the initial setting of the field is coherent. For coherent field C_k in (10) represents the number-state expansion coefficients $C_k = \langle n|\psi_F(0)\rangle$, so for coherent state

$$C_k = \exp(-|\alpha|^2/2)\alpha^n/\sqrt{n!}; \quad \alpha = |\alpha|e^{i\xi}, \tag{55}$$

where $|\alpha|^2 = \langle n\rangle = \bar{n}$ is the mean photon number in the initial state. The photon distribution for coherent state given by

$$p(n) = \exp(-|\alpha|^2)\frac{(|\alpha|^2)^n}{n!}, \tag{56}$$

which is always peak at $n_{peak} = |\alpha|^2 = \langle n\rangle = \bar{n}$.

For the case under consideration, the field entropy S_F as well as P as a functions of λt were plotted versus the scaled time $\lambda t/\pi$ in Figs. 8–11 according to the complex amplitudes (17)–(22) for atomic motion $v = \lambda L/\pi$. For all our plots the initial condition has been chosen with real α such that the mean photon number $\bar{n} = 10$. To visualize the effect of the atomic motion and the field-mode structure parameter p on the entanglement dynamics, we have Fig. 8 contains temporal evolution of both S_F and P for different values of

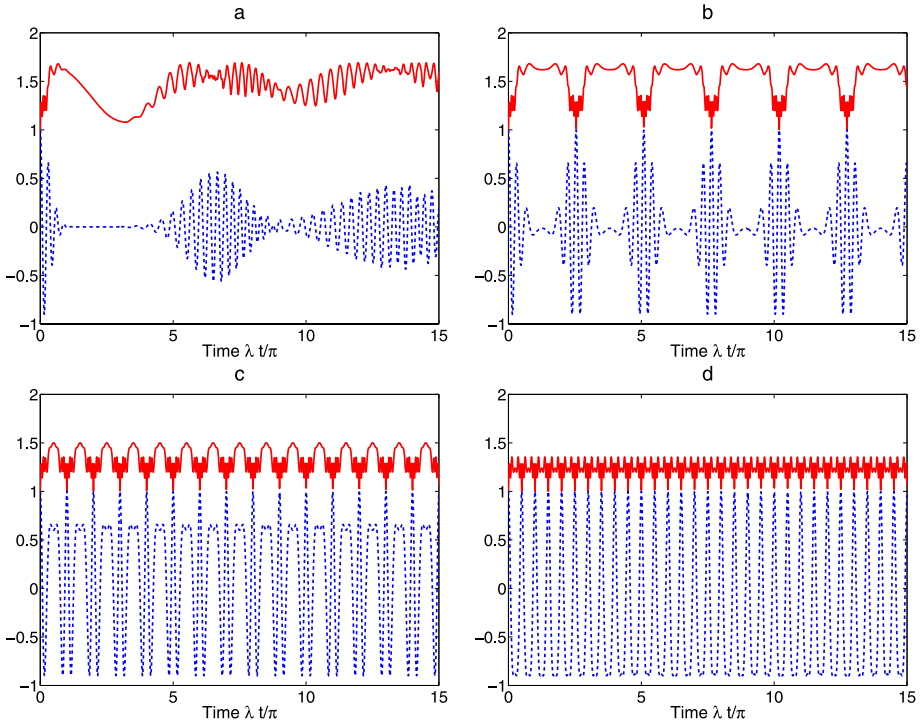

Fig. 8 The time evolution of field entropy $S_F(t) + 1$ (*solid line*) and the population $P(t)$ (*dashed line*) as functions of the scaled time λt where the field is excited initially in the coherent state with mean photon number $\bar{n} = 10$, where (**a**) $p = 0$, (**b**) $p = \pi/8$, (**c**) $p = 1$ and (**d**) $p = 2$

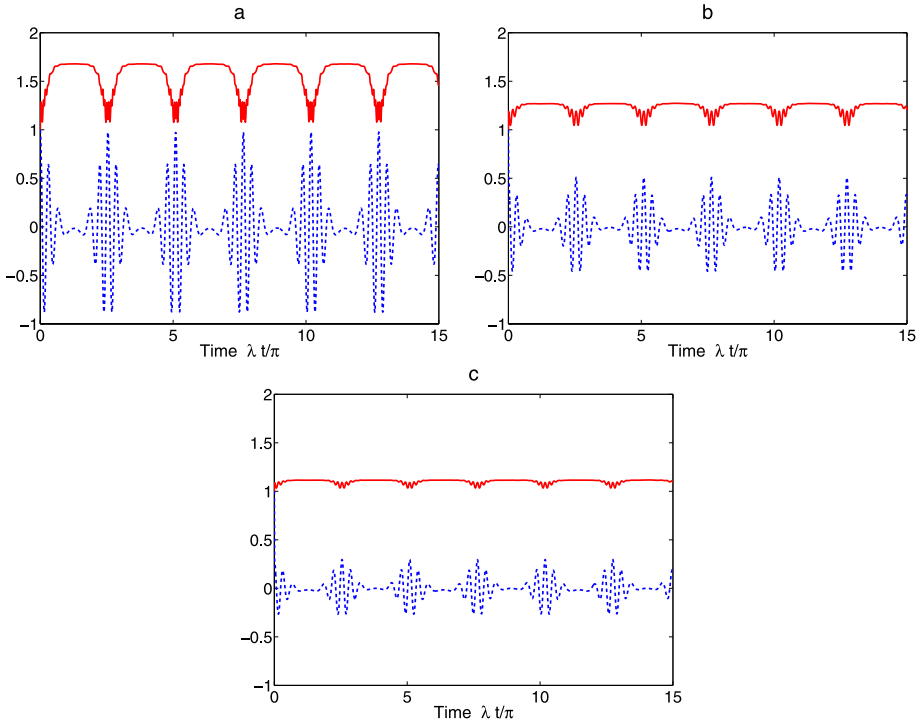

Fig. 9 The time evolution of field entropy $S_F(t)+1$ (*solid line*) and the population $P(t)$ (*dashed line*) as functions of the scaled time λt where the field is excited initially in the coherent state with mean photon number $\bar{n}=10$ and the field-mode structure $p=\pi/8$ where (**a**) $\chi/\lambda=0.05$, (**b**) $\chi/\lambda=0.5$ and (**c**) $\chi/\lambda=1.0$

the parameter p where the nonlinear Kerr-like medium is neglected. For rest atoms, one purely notice the well known temporal evolution of both S_F and P [4, 51], where the first maximum of the field entropy at $\lambda t>0$ is achieved at the collapse time. Furthermore, the atom-field system returns most closely to a disentangled interaction sometimes during the collapse region. Additionally, at near the center of the collapse region, at half of the atomic inversion revival time $t_R=2\pi\sqrt{\bar{n}}/\lambda=\frac{10\pi}{\lambda}$, the entropy reaches its local minimum. During subsequent collapses the field approaches the disentangled state from the atom at times $t_n=(2n+1)\sqrt{\bar{n}}\pi/\lambda$, $n=0,1,2,3,\ldots$. Also, it can been seen that the behaviors of S_F and P are not periodical for the atom at rest.

The influences of the atomic motion and the field-mode structure on the S_F and P for different values of p can be seen in Figs. 8b–d. As seen form these figures, we can conclude that the atomic motion leads to the periodic evolution of both the entropy S_F and the population P. The periods lay at $\lambda t=\frac{5n\pi}{2}$; $n=0,1,2,3,\ldots$ for $p=\pi/8$ (see Fig. 8b). Physically, all these features can be attributed to the change in the atom-field interaction time due to the atomic motion. This is due to the fact that the complex amplitudes a_k and b_{k+1} in the two cases result from the time functional dependence and so does the quantities ρ_{kl} and ρ_{k+1l+1} on which the entropy and the population depend crucially. When the atomic motion is ignored, the time factor is the scaled time λt, and the complex amplitudes are then $a_k(\lambda t)$ and $b_{k+1}(\lambda t)$ and so $\rho_{kl}(\lambda t)$ and $\rho_{k+1l+1}(\lambda t)$, while it is $\lambda\Theta(t)=\frac{1}{p\lambda}\sin(p\lambda t)$ when the atomic motion is considered, and then the complex amplitudes become $a_k[\lambda\Theta(t)]$ and $b_{k+1}[\lambda\Theta(t)]$ and so $\rho_{kl}[\lambda\Theta(t)]$ and $\rho_{k+1l+1}[\lambda\Theta(t)]$. The evolution behavior of S_F and P can

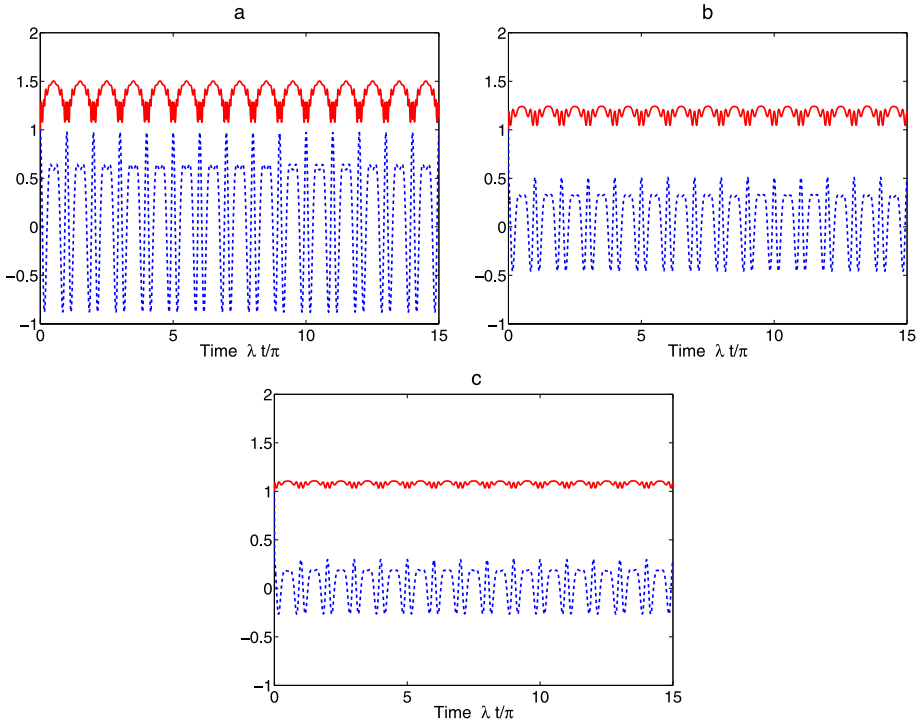

Fig. 10 The same as Fig. 9 but for $p = 1$

be understood simply by considering the relation between the scaled time λt and $\lambda\Theta(t)$. It is observed that $\lambda\Theta(t)$ is a periodical function on the scaled time λt with period $2\pi/p$. This periodicity of $\lambda\Theta(t)$ of the scaled time λt just leads to the periodicity of the evolution of S_F and P. When the parameter p begin increasing, rapid oscillations between zeros and maxima of both S_F and P with considerable reduction of the amplitudes of S_F depends crucially on the value of p, where the higher the value of p, the smaller the amplitudes of both S_F and P, while the maxima of P remain fixed with more rapid oscillation as p increases. It is worth to mention that the periodic behavior is still reserved. The periods lay at $\lambda t = \frac{n\pi}{5}$; $n = 0, 1, 2, 3, \ldots$, where the periods of the oscillations become more closer (see Fig. 8c where $p = 1$). It is not difficult to notice that the locations of maxima and minima of both S_F and P become closer and closer with the increase of p (see Fig. 8d where $p = 2$). Let us now come to specific numerical examples to investigate the influence of the atomic motion, the field-mode structure and the Kerr medium on the evolution of both the field entropy S_F and the population P. The numerical calculations are depicted in Figs. 9–11 according to the complex amplitudes (20)–(22) versus the Rabi angle $\lambda t/\pi$, where we consider the effect of several values of the Kerr medium parameter χ/λ in the presence of different shapes of the field-mode structure. One can distinguish clearly between the evolution stages of S_F and P on Kerr medium going to strength. Each of these stages has been pictured separately. It is important to note that the nonlinear interaction of the Kerr medium with the field mode is very weak for $\chi/\lambda = 0.05$. We notice that the weak nonlinear interaction of the Kerr medium with the field mode leads to increasing values of the entropy maxima and minima and increasing of the sustainment time of maximum entropy. In this case the field and the

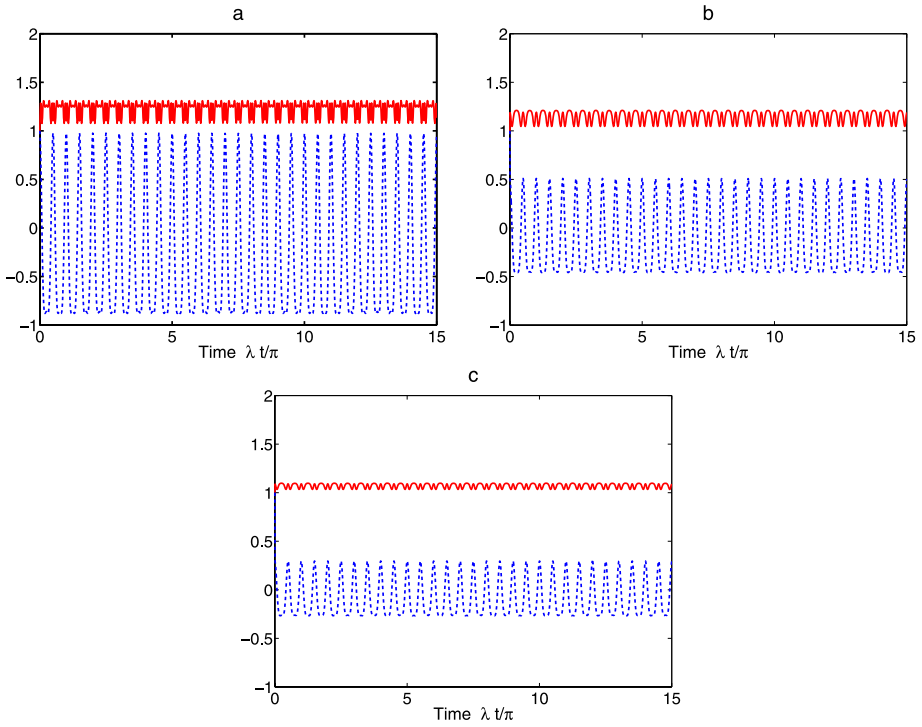

Fig. 11 The same as Fig. 9 but for $p = 2$

atom almost retain a strong entanglement in the time evolution process (see Fig. 9a) for longer periods of time. With the increase of the nonlinear interaction of the Kerr medium with the cavity mode, the values of both the maximum and minimum field entropy begins to decrease. In this case the degree of maximum entanglement between the field and the atom reduces while they remain entangled weakly. We note that the amplitudes of the field entropy decreases as χ/λ increases (Figs. 10 and 11). It is evident that the field and the atom are almost in entangled states when the Kerr medium effect increases. This result violate the fact that in the limit of very strong nonlinear interaction of the Kerr medium with the field mode, the field and the atom are almost decoupled, which preserves the field entropy tending to zero. Physically, all these features can be attributed to the change in the atom-field interaction time due to the atomic motion. It is worth to mention that, in all stages the field entropy and the population do not lose periodicity at all. Furthermore, the presence of the atomic motion changes the well known influence of the Kerr medium on the field entropy $S_F(t)$ and the population $P(t)$, where with initially coherent state field the Kerr medium results in decoupling of the atom-field system [54, 55]. Also, the noticed effect of creating periodicity by the atomic motion either with or without Kerr medium.

6 Conclusion

The (JC) model has been extended to incorporate the effects of atomic motion, field-mode structure and Kerr-like medium. The analytical form of the system state vector has been

obtained. We examined the effects of the atomic motion, the field-mode structure and the Kerr-like medium on the dynamics of entropy of entanglement of the cavity and atomic populations. Two classes of initial excitations of the cavity were considered, namely, a Fock state and a coherent state. The results showed that the presence of both atomic motion, field-mode structure and the Kerr medium plays an essential role in the evolution of the field entropy and atomic population dynamics. We can conclude as follows.

First: generally regardless of the initial type of the cavity excitation, the atomic motion leads to a periodic evolution of the field entropy and atomic populations. Periodicity neither depends at all on the statistics distribution nor the intensity of excitation, but on the atomic velocity v, the length of the cavity L and the field-mode structure parameter p.

Second: (i) in case of an excited cavity in a Fock state, high degree of entanglement with maximum fixed strength without decays or nodes at zero can be achieved with strong Kerr medium regardless of the value of the field-mode structure parameter when $p > 0$.

(ii) When the cavity is excited in a coherent state—in case of strong Kerr medium—the presence of atomic motion and field-mode structure parameter does not change the general well-known negative effect of the Kerr medium on the degree of entanglement except for the periodical behavior. The weak Kerr medium leads to the increase of values of minimum entropy and the sustainment time of the maximum entropy. Although the Kerr medium affects the strength of the entanglement negatively, the entropy of entanglement loses its zeros as the Kerr is taken into account.

Acknowledgements The Author would like to thank the referees for helpful and constructive comments and suggestions that actually helped to improve the article text in many ways.

References

1. Wu, Y., Yang, X.: Phys. Rev. A **56**, 2443 (1997)
2. Joshi, A., Lawanda, S.V.: Int. J. Mod. Phys. B **6**, 3539 (1992)
3. Joshi, A., Lawanda, S.V.: Phys. Rev. A **42**, 1752 (1990)
4. Schlicher, R.R.: Opt. Commun. **70**, 97 (1989)
5. Liu, T.K., Wang, J.S., Zhan, M.S.: Chin. J. At. Mol. Phys. **18**, 58 (2001)
6. Walls, D.F., Milburn, G.J.: Quantum Optics. Springer, Berlin (1994)
7. Liu, X.-J., Zhou, B.-J., Liu, M.-W., Li, S.-C.: Chin. Phys. **16**, 3685 (2007)
8. Hu, Y.-H., Fang, M.-F., Liao, X.-P.: Chin. Phys. **16**, 1344 (2007)
9. Fang, M.-F.: Physica A **259**, 193 (1998)
10. Schrödinger, E.: Proc. Camb. Philos. Soc. **31**, 555 (1935)
11. Einstein, A., Podolsky, B., Rosen, N.: Phys. Rev. **47**, 777 (1935)
12. Nielsen, M., Chang, I.: Quantum Computation and Quantum Communication. Cambridge University Press, Cambridge (2000)
13. Bennett, C.H., Brassard, G., Crépeau, C., Jozsa, R., Peres, A., Wootters, W.K.: Phys. Rev. Lett. **70**, 1895 (1993)
14. Bennett, C.H., Brassard, G., Vepeau, C.: Phys. Rev. Lett. **70**, 1895 (1993)
15. Bennett, C.H., Brassard, G., Mermin, N.D.: Phys. Rev. Lett. **68**, 557 (1992)
16. Ekert, A.: Phys. Rev. Lett. **67**, 661 (1991)
17. Bennett, C.H., Wiesner, S.J.: Phys. Rev. Lett. **69**, 2881 (1992)
18. Bennett, C.H.: Phys. Today **48**, 24 (1995)
19. Bennett, C.H., DiVincenzo, D.P.: Nature **404**, 247 (2000)
20. Ma, J.-M., Jiao, Z.-Y., Li, N.: Int. J. Theor. Phys. **46**, 2550 (2007)
21. Zhang, X.-T., Zhu, A.-D., Zhang, S.: Chin. Phys. Lett. **24**, 1460 (2007)
22. Wang, C.-Z., Li, C.-X., Guo, G.-C.: Eur. Phys. J. D **37**, 267 (2006)
23. Yu, C.-S., Song, H.-S.: quant-ph/0603038v1 (2006)
24. Klich, I., Refael, G., Silva, A.: quant-ph/0603004v1 (2006)
25. Mintert, F., Buchleitner, A.: quant-ph/0411130v1 (2004)
26. Santos, M.F., Milman, P., Davidovich, L., Zagury, N.: quant-ph/0509204v2 (2006)

27. Mintert, F., Kuś, M., Buchleitner, A.: quant-ph/0411127v1 (2004)
28. Boukobza, E., Tannor, D.J.: quant-ph/0505119v1 (2005)
29. Heydari, H., Björk, G.: quant-ph/0410124v1 (2004)
30. Gour, G.: quant-ph/0506229v2 (2005)
31. Peters, N.A., Wei, T.-C., Kwiat, P.G.: Phys. Rev. A **70**, 052309 (2004)
32. Bennett, C.H., Bernstein, H.J., Popescu, S., Schumacher, B.: Phys. Rev. A **53**, 2046 (1996)
33. Bennett, C.H., DiVincenzo, D.P., Smolin, J.A., Wootters, W.K.: Phys. Rev. A **54**, 3824 (1996)
34. Vedral, V., Plenio, M.B.: Phys. Rev. A **57**, 1619 (1996)
35. Vedral, V.: Rev. Mod. Phys. **74**, 197 (2002)
36. Abdel-Aty, M.: Prog. Quantum. Electron. **31**, 1 (2007)
37. Vidal, G., Tarrach, R.: Phys. Rev. A **59**, 141 (1999)
38. Joshi, A., Puri, R.R.: Phys. Rev. A **45**, 5056 (1992)
39. Hillery, M.: Phys. Rev. A **44**, 4578 (1991)
40. Chaba, A.N., Collett, M.J., Walls, D.F.: Phys. Rev. A **46**, 1499 (1992)
41. Zambrini, R., Hoyuelos, M., Gatti, A., Colet, P., Lugiato, L., Miguel, M.S.: Phys. Rev. A **62**, 063801 (2000)
42. Gerry, C.C.: Phys. Rev. A **59**, 4095 (1999)
43. Paternostro, M., Kim, M.S., Ham, B.S.: Phys. Rev. A **67**, 023811 (2003)
44. Pachos, J., Chountasis, M.: Phys. Rev. A **62**, 052318 (2000)
45. Vitali, D., Fortunato, M., Tombesi, P.: Phys. Rev. Lett. **85**, 445 (2000)
46. Ateto, M.S.: Int. J. Quant. Inf. **5**, 535 (2007)
47. Zhang, X.-T., Zhu, A.-D., Zhang, S.: Chin. Phys. Lett. **24**, 1460 (2007)
48. Wang, C.-Z., Li, C.-X., Guo, G.-C.: Eur. Phys. J. D **37**, 267 (2006)
49. Sargent, M. III, Scully, M.O., Lamb, W.E., Jr.: Laser Physics. Addison-Wesley, Reading (1974)
50. Bartzis, V.: Physica A **180**, 428 (1992)
51. Phoenix, S.J.D., Knight, P.L.: Phys. Rev. A **44**, 6023 (1991)
52. Phoenix, S.J.D., Knight, P.L.: Phys. Rev. Lett. **66**, 2833 (1991)
53. Phoenix, S.J.D., Knight, P.L.: Ann. Phys. NY **186**, 381 (1988)
54. Abdel-Aty, M., Furuichi, S., Ateto, M.: Jpn. J. Appl. Phys. **41**, 111 (2002)
55. Abdel-Aty, M.: J. Phys. B: At. Mol. Opt. Phys. **33**, 2665 (2000)
56. Buzek, V., Jex, I.: Opt. Commun. **78**, 425 (1990)